This full text paper was peer reviewed at the direction of IEEE Communications Society subject matter experts for publication in the WCNC 2008 proceedings.

Joint Impact of Quantization and Clipping on Single- and Multi-carrier Block Transmission Systems

Haibing Yang[1], Tim C. W. Schenk[2], Peter F. M. Smulders[1] and Erik R. Fledderus[1,3]
[1]Eindhoven University of Technology, Radio Communications Group (TTE-ECR), Eindhoven, The Netherlands
[2]Philips Research, Distributed Sensor Systems Department, Eindhoven, The Netherlands
[3]TNO Information and Communication Technology, Delft, The Netherlands
Email: h.yang@tue.nl

***Abstract*—This work investigates the joint impact of quantization and clipping, caused by analog-to-digital converters (ADCs) with low bit resolutions, on single- and multi-carrier block transmission systems in wireless multipath environments. We consider single carrier block transmission with frequency domain equalization (SC-FDE) and the multi-carrier techniques OFDM and MC-CDMA. By approximating the ADC input as Gaussian distributed, the effective signal-to-noise ratio in the received signal and decision variables are derived and analyzed. The bit-error rate (BER) performance is simulated and compared for various constellations under different multipath conditions. The results reveal that frequency diversity is an effective measure to combat the joint impact of quantization and clipping. For the ADCs with moderate resolution bits, i.e., R = 5 and 4 bits, SC-FDE is shown to achieve the same performance as MC-CDMA. It is noted that due to the applied Gaussian approximation for the received signals, the derived SC-FDE results provide a lower bound on the performance of the systems under the influence of the ADC nonlinearity. This bound is tight, however, in case of rich multipath environments.**

I. Introduction

The analog-to-digital converter (ADC) is a critical component in modern digital wireless communication systems. With the ever increasing data rate requirements, currently studied wireless systems, such as the ultra-wideband (UWB) and 60 GHz radio applications in wireless personal area networks (WPAN) [1], [2], will occupy a broadband spectrum bandwidth as wide as several GHz and the throughput will be in the order of Gb/s. To realize the resulting high sampling rate and meanwhile keep the power consumption low, it is desired to apply an ADC with a very low bit resolution. With the reduced resolution, however, the signal distortion at the ADC output will become serious and eventually it will degrade the system performance.

The nonlinear effect due to the ADC component has been widely studied by modelling the ADC output as the input signal plus its distortion [3]. For a high bit resolution ADC, the distortion noise may be assumed to be uniformly distributed and uncorrelated with the input signal [4], [5]. For a low bit resolution, however, this traditional model is inaccurate, since the distortion becomes highly correlated with the input signal due to the large clipping noise in addition to the quantization noise[1]. In contrast to the traditional model, a more accurate model for a memoryless ADC is to decompose the output, according to the generalized Bussgang's theorem by Nuttall [6], into an attenuated input signal plus a distortion component that is uncorrelated with the ADC input. For any static memoryless nonlinear device, this new model is valid for a wide class of input signal if and only if the input is a separable stochastic process. By using this model, accurate signal-to-noise ratio (SNR) information can be provided for signal detection in the receiver. This model has been applied in [7] to evaluate and optimize the clipping and quantization effect for a Gaussian input signal.

To achieve high data rate transmission, block transmission systems, in which guard intervals are inserted between data blocks, have been widely accepted for many applications in modern wireless communication systems [8]–[10]. The class of the block systems is advantageous to effectively avoid inter-block interference and to efficiently apply frequency domain equalization (FDE). In general, the block transmission systems can be divided into two categories: multi-carrier schemes, such as orthogonal frequency division multiplexing (OFDM) and multi-carrier code division multiple access (MC-CDMA), and single carrier transmission schemes, such as single carrier block transmission with FDE (SC-FDE).

A multi-carrier signal typically has a higher peak-to-average power ratio (PAPR) than a single carrier signal. Therefore, the impairments caused by channel nonlinearities might be more serious in multi-carrier transmissions. In literature, single- and multi-carrier schemes are often compared under the effect of nonlinear impairments introduced at the transmitter side [11], but they are rarely compared under the nonlinear ADC effect at the receiver side. The ADC effect on OFDM transmission has been considered in [12], [13], based on the traditional ADC model, and in [7], based on the new ADC model. MC-CDMA is based on the OFDM technique and suitable for multi-user application, but essentially different from OFDM in that frequency diversity is inherently utilized. The SC-FDE scheme utilizes frequency diversity as well, but the signals have a lower PAPR.

Hence, due to the difference in the frequency diversity and PAPR, the following question arises: how will the performance of these transmission schemes differ when an ADC with limited resolution is used? To answer the question, this paper analyzes the system behaviors and compares the transmission

[1]Here the quantization noise and clipping noise correspond to the granular noise and overloading distortion, respectively, in literature [4].

1525-3511/08/$25.00 ©2008 IEEE

performance of the three schemes by regarding the joint effect of ADC-caused quantization and clipping. With the aid of the new statistical ADC model, the decision variables are derived. Moreover, simulations are conducted to compare the system performance for various constellations under different multipath channel conditions.

II. System model and analysis

A. System model

The basic principle of OFDM is to divide the available bandwidth into multiple narrowband subcarriers and to modulate each subcarrier with a user data stream at a lower symbol rate. The user symbols are then transmitted block by block and a cyclic prefix is often inserted between blocks to absorb interferences between blocks. MC-CDMA is based on the OFDM technique, but user symbols are spread over multiple subcarriers with the aid of a spreading code, such as the Walsh-Hadamard code, before the IFFT operation. For SC-FDE, user symbols are transmitted block by block at a single carrier and cyclic prefixes are inserted in a similar way as in OFDM.

For the three schemes, equalization in the receiver can be conducted in the frequency domain to compensate the complex attenuation caused by the channel before demodulation. Because of the similarities in block transmission and FDE, the three schemes can be incorporated into one structure as shown in Fig. 1. One can check that when the (de)spreading code matrix is implemented as an identity matrix $\boldsymbol{I}$, an (inverse) Walsh-Hadamard (WH) matrix $\boldsymbol{C}$ or an (inverse) Fourier matrix $\boldsymbol{F}$, the transceiver structure becomes OFDM, MC-CDMA or SC-FDE, respectively.

Here we describe the general structure of the transceiver system in detail, where $\boldsymbol{C}$ represents a possible code spreading matrix. In the transmitter, user symbols are packed into data blocks with length N and each block is linearly transformed by a code spreading matrix before an IFFT operation. For convenience, we only consider one block denoted as $\boldsymbol{x} = [x_0, x_1, \cdots, x_{N-1}]^T$, where the data symbols are zero mean, independent and identically-distributed (i.i.d.) with variance E_s, i.e. $\mathbb{E}\{\boldsymbol{x}\boldsymbol{x}^H\} = E_s\boldsymbol{I}$. After code spreading and the IFFT, the resulting signal block is given by

$$\boldsymbol{u} = \boldsymbol{F}^H\boldsymbol{C}\boldsymbol{x}, \tag{1}$$

with $\boldsymbol{u} = [u_0, u_1, \cdots, u_{N-1}]^T$, ^{H} denotes the complex transpose and $\boldsymbol{F}$ is the $N \times N$ Fourier matrix with the (k,l)th entry $F_{k,l} = \frac{1}{\sqrt{N}} e^{-\imath 2\pi kl/N}$ and $\imath = \sqrt{-1}$. In case of MC-CDMA, $\boldsymbol{C}$ is a WH matrix performing code spreading operation and built with the elements $C_{m,n} = \frac{1}{\sqrt{N}} \prod_{i=0}^{N-1} (-1)^{m_i n_i}$, where $m = \sum_{i=0}^{N-1} m_i 2^i$, $n = \sum_{i=0}^{N-1} n_i 2^i$ and $m_i, n_i \in \{0,1\}$ are the binary representations of m and n, respectively.

After the IFFT, a cyclic prefix is placed in the front of the signal block and then the signal block is transmitted in a time-invariant multipath dispersive channel with channel length L+1. Without loss of generality, we assume that the length of the cyclic prefix is always larger than the channel length. In this way, the inter-block interference can be completely resolved by the cyclic prefix.

In the receiver, we assume that the time and frequency synchronization of the signal are perfect and that the cyclic prefix is removed. Then the received signal block before the FFT is $\boldsymbol{r} = [r_0, r_1, \cdots, r_{N-1}]^T$, in which the entries are the circular convolution of the transmitted signal and the channel impulse response contaminated by noise, i.e.

$$r_n = \sum_{l=0}^{L} h_l u_{(n-l) \bmod N} + \hat{v}_n. \tag{2}$$

Here $\{h_l\}$ are the taps of the channel impulse response and $\{\hat{v}_n\}$ are zero mean i.i.d. additive white Gaussian noise (AWGN) with variance N_0. For a Rician fading channel, the first tap h_0 is fixed and other taps are i.i.d. complex Gaussian distributed, where the Rician K-factor is defined by $K = \frac{\mathbb{E}\{|h_0|^2\}}{\mathbb{E}\{\sum_{l=1}^{L} |h_l|^2\}}$. For convenience, the channel power is normalized, i.e., $\mathbb{E}\left\{\sum_{l=0}^{L} |h_l|^2\right\} = 1$, and the average SNR of the received signal thus equals $\overline{\gamma} = \frac{E_s}{N_0}$. Rewriting (2) into vector form leads to

$$\boldsymbol{r} = \mathrm{cir}\{\boldsymbol{h}\}\boldsymbol{u} + \hat{\boldsymbol{v}}, \tag{3}$$

where the noise $\hat{\boldsymbol{v}} = [\hat{v}_0, \hat{v}_1, \cdots, \hat{v}_{N-1}]^T$ and the channel matrix $\mathrm{cir}\{\boldsymbol{h}\}$ is an $N \times N$ circulant matrix with the first column vector $\boldsymbol{h} = [h_0, h_1, \cdots, h_L, 0, \cdots, 0]^T$.

The received signal after applying the FFT to $\boldsymbol{r}$, the signal may be written as

$$\boldsymbol{y} = \boldsymbol{H}\boldsymbol{C}\boldsymbol{x} + \boldsymbol{v}, \tag{4}$$

where $\boldsymbol{y} = [y_0, y_1, \cdots, y_{N-1}]^T$, the noise vector $\boldsymbol{v} = \boldsymbol{F}\hat{\boldsymbol{v}}$ and the channel matrix in frequency domain $\boldsymbol{H} = \boldsymbol{F}\mathrm{cir}\{\boldsymbol{h}\}\boldsymbol{F}^H$. Since the channel considered in this paper is time invariant, it can be proved that the matrix $\boldsymbol{H}$ is diagonal and the nth diagonal element, $H_n = \sum_{k=0}^{N-1} h_k e^{-\imath 2\pi kn/N}$, represents the complex attenuation of the channel at the nth subcarrier.

B. MMSE equalization and decision variables

To equalize the signal attenuation and rotation caused by the channel at each subcarrier, the received signal vector $\boldsymbol{y}$ is weighted by a diagonal matrix $\boldsymbol{W} = \mathrm{diag}\{[W_0, W_1, \cdots, W_{N-1}]^T\}$ prior to the code despreading and symbol detection. After equalization, the despreading of the equalized signal leads to the vector of decision variables given by

$$\boldsymbol{s} = \boldsymbol{C}^H\boldsymbol{W}\boldsymbol{y} = \boldsymbol{C}^H\boldsymbol{W}\boldsymbol{H}\boldsymbol{C}\boldsymbol{x} + \boldsymbol{C}^H\boldsymbol{W}\boldsymbol{v}, \tag{5}$$

which are then fed into a detection device for the recovery of the user data symbols. The choice of the weight W_n depends on the performance criteria. A minimum mean-square error (MMSE) equalizer compromises the noise enhancement and signal distortion, and eventually achieves the best performance among linear equalizers. Therefore, the MMSE equalizer will be considered in the rest of the paper. In this case, the nth weight is $W_n = \frac{\overline{\gamma} H_n^*}{\overline{\gamma}|H_n|^2 + 1}$, where * denotes conjugate.

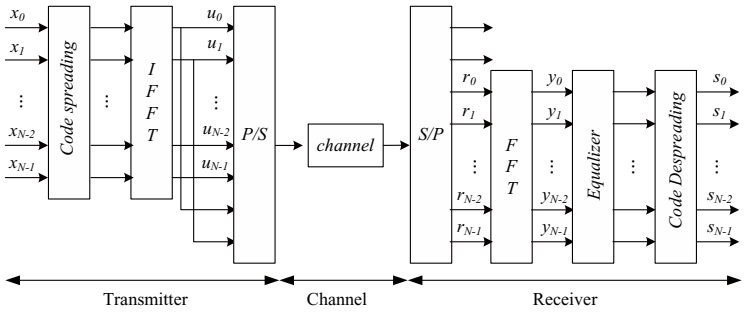

Fig. 1. Baseband equivalent transceiver system.

For an OFDM system where $\boldsymbol{C} = \boldsymbol{I}$, the nth decision variable within one data block and its instantaneous SNR can be expressed by

$$s_n = \frac{\overline{\gamma}|H_n|^2}{\overline{\gamma}|H_n|^2+1}\cdot x_n + \frac{\overline{\gamma}H_n^*}{\overline{\gamma}|H_n|^2+1}\cdot v_n, \quad (6)$$

$$\gamma_n = \overline{\gamma}|H_n|^2, \quad (7)$$

respectively, for the MMSE equalizer.

For both SC-FDE and MC-CDMA, the expression of the nth decision variable within one data block is a bit more complex than the one for OFDM in (6) and it is given by

$$s_n = \beta x_n + e_n, \quad (8)$$

where $\beta = \frac{1}{N}\sum_{k=0}^{N-1}\frac{\overline{\gamma}|H_k|^2}{\overline{\gamma}|H_k|^2+1}$ is the scaling factor of the desired signal and e_n is the error signal given by

$$e_n = \sum_{\substack{m=0\\m\neq n}}^{N-1} x_m \sum_{k=0}^{N-1}\frac{C_{kn}^* C_{km}|H_k|^2}{|H_k|^2+1/\overline{\gamma}} + \sum_{m=0}^{N-1}\frac{C_{nm}H_m^*}{|H_m|^2+1/\overline{\gamma}}\cdot v_m. \quad (9)$$

The error signal consists of the residual inter-symbol-interference (ISI) in the first term and the correlated noise in the second term. The error signal occurs since the signal and noise component at different subcarriers are combined into the decision variable either by the IFFT operation in SC-FDE or the WH code despreading operation in MC-CDMA, respectively. After some manipulations, the variance of the error signal can be derived to equal $\beta(1-\beta)$. From (8), one can check that the instantaneous SNRs of the decision variables in SC-FDE and MC-CDMA are exactly the same for all n and are given by the expression

$$\eta = \frac{1}{\frac{1}{N}\sum_{n=0}^{N-1}\frac{1}{\overline{\gamma}|H_n|^2+1}} - 1. \quad (10)$$

According to (10), both SC-FDE and MC-CDMA should achieve the same detection performance, due to the same SNR for the decision variable. Therefore, we conclude that the two schemes are essentially the same, though it is more convenient to apply MC-CDMA into multi-user applications.

In case of a flat fading channel, i.e., $|H_n|^2 = 1$ for any n, the three schemes achieve exactly the same performance since $\gamma_n = \eta = \overline{\gamma}$. In case of a frequency selective channel, compare (7) and (10), one can see that for OFDM, the data symbol carried by certain subchannels with deep fades might not be detected correctly. For SC-FDE and MC-CDMA, in contrast, such deep fades do not have such a big impact since each data symbol has been spread over all the subchannels. When the SNR of the received signal is at a certain low level, however, SC-FDE and MC-CDMA might not have any correct detection at all, since all decision variables experience the same SNR. OFDM may still recover the symbols carried by the subchannels with sufficiently high SNRs in this case.

III. Nonlinear effect of the ADC converter

A. ADC model and quantization interval

For a R bit resolution ADC with $M = 2^R$ quantization levels, the real output Y and the real input X of an ADC are related by the quantization function Q, defined as

$$Y = Q(X) = \sum_{m=-\frac{M}{2}+1}^{m=\frac{M}{2}} Y_m \cdot U(X, \hat{X}_{m-1}, \hat{X}_m), \quad (11)$$

where $\hat{X}_m$ represents the mth quantization threshold value, Y_m is the output amplitude of the mth quantization interval and $U(X,a,b)$ is the rectangular function defined as

$$U(X,a,b) = \begin{cases} 1, & a \le X < b \\ 0, & \text{otherwise.} \end{cases} \quad (12)$$

In the case of the commonly used mid-raiser uniform quantization with the step size Δ, the quantization threshold and the output amplitude are given by

$$\hat{X}_m = \begin{cases} m\Delta & |m| < M/2 \\ -\infty & m = -M/2 \\ +\infty & m = M/2 \end{cases}, \quad (13)$$

$$Y_m = m\Delta - \Delta/2, \quad (14)$$

respectively. Signal distortion at the ADC output consists of the quantization error and the clipping error, which occur when the input signal is within or out of the range of $[-\frac{M\Delta}{2}, \frac{M\Delta}{2}]$, respectively.

According to the generalized Bussgang's theorem in [6], if the input signal X of the nonlinear memoryless ADC is a separable random process[2], the output signal Y can be

[2]Separability of a process here means that the conditional expectation of an input signal $X(t)$ should satisfy $\mathbb{E}\{X(t-\tau)|X(t)\} = \frac{R_X(\tau)}{R_X(0)}\cdot X(t)$, where $R_X(\tau)$ is the covariance of $X(t)$. The separability is valid for a number of signals, e.g. Gaussian processes and phase modulated processes [6].

decomposed into

$$Y = \alpha X + D, \tag{15}$$

where α is a scaling factor and D is a distortion term, which is uncorrelated with X. The distortion D, caused by the quantization and clipping of the ADC, is generally non-Gaussian and has the variance $\sigma_D^2 = \sigma_Y^2 - \alpha^2\sigma_X^2$, where σ_X^2 and σ_Y^2 are the variances of the ADC input and output, respectively. The scaling factor can be derived by $\alpha = \frac{1}{\sigma_X^2}\int_{-\infty}^{\infty} XQ(X)p_X(X)dX$, where $p_X(X)$ is the pdf of X. Now the signal-to-distortion ratio (SDR) at the ADC output can be expressed by $\text{SDR} = \frac{\alpha^2\sigma_X^2}{\sigma_D^2}$. For a certain distribution of the I/Q signal, the optimal quantization interval Δ can be chosen such to maximize SDR at the ADC output. This is, however, a complicated design procedure since the distributions of the received signal depend not only on the transmit signal but also on the experienced channel.

Consider that the I and Q branches of the received signal (2) are quantized by a pair of the ADCs as defined in (11) with R bit resolution. Note that the received signal consists of a linear combination of data symbols, which are zero mean complex i.i.d. random variables with variance E_s, due to the code spreading (in case of MC-CDMA), IFFT (in case of OFDM and MC-CDMA) and multipath dispersions, in addition to the AWGN noise in the receiver. According to the central limit theorem, the I/Q signals of the three schemes approach zero mean Gaussian distributions with variance $\sigma_X^2 = (E_s+N_0)/2$, for a large number of multipaths. Therefore, it is reasonable to set the quantization interval in this paper to be the values which are optimally chosen for Gaussian inputs. The intervals are, for instance, $\Delta_{\text{opt}} \approx \sigma_X[0.5860, 0.3352, 0.1881]$ for $R = 3, 4$ and 5 bits, respectively [7]. For Gaussian inputs of the ADC and these intervals, the scaling factors $\alpha_{\text{opt}} = 0.9626, 0.9885, 0.9965$ and the maximum SDRs are achieved, given by $\text{SDR}_{\text{opt}} = 14.10, 19.33, 24.55$ dB.

B. ADC effect on block transmission schemes

According to (15), the complex ADC output signal is the linearly scaled version of (3) plus an uncorrelated distortion term. The FFT operation leads to the frequency domain ADC output

$$\tilde{\boldsymbol{y}} = \alpha(\boldsymbol{HCx} + \boldsymbol{v}) + \boldsymbol{d}, \tag{16}$$

where $\boldsymbol{d}$ is the distortion in the frequency domain with variance σ_d^2 for each element. The distortion is uncorrelated with the signal $\boldsymbol{x}$ and the channel noise $\boldsymbol{v}$. By incorporating the scaling factor into the channel attenuation and the distortion into the channel noise, the average SNR at the ADC output becomes $\widetilde{\gamma} = \frac{\alpha^2 E_s}{\alpha^2 N_0 + \sigma_d^2}$ and may be further simplified as

$$\widetilde{\gamma} = \frac{\overline{\gamma}}{1 + \frac{\overline{\gamma}+1}{\text{SDR}}} \tag{17}$$

by using $\frac{\sigma_d^2}{\alpha^2} = \frac{E_s+N_0}{\text{SDR}}$ and $\overline{\gamma} = \frac{E_s}{N_0}$. Notice that the SDR values are different for the three transmission schemes, i.e. , it depends on the received signal distributions.

For the multi-carrier transmission schemes, both the transmitted and received I/Q signal can be well approximated by Gaussian distributions. These distributions are relatively insensitive to the actual multipath channel. This is reflected in the relatively high PAPR levels, as studied in Section IV-B, as compared to SC-FDE. As a result, the SDR in (17) approaches SDR_{opt} derived in Section III-A.

In contrast, the signal distribution for SC-FDE depends not only on the channel conditions but also on the applied transmit constellations. More specifically, the I/Q signal distribution resembles the Gaussian distribution for severe multipath environments, but not in near-flat fading channels especially for lower-order constellations. In any case, the signal distribution of SC-FDE will have much shorter tails than those of the multi-carrier signals, which leads to a lower PAPR. Consequently, the SC-FDE signal at the ADC output has the least clipping error among the three schemes for the same quantization interval. Hence, this leads to the largest SDR and, eventually, the largest effective SNR at the ADC output.

Now replacing $\overline{\gamma}$ in (7) and (10) by $\widetilde{\gamma}$ leads to the effective SNRs of decision variables for the three transmission schemes. In comparison with SC-FDE and MC-CDMA, the SNR loss in OFDM caused by the ADC is directly imposed on each decision variable, which might result in even worse detection performance in frequency selective channels. In addition, SC-FDE and MC-CDMA might have a similar effective SNR in decision variables, which indicates a similar BER performance, when the clipping errors are ignorable or have the same level.

IV. PAPR AND BER EVALUATION FOR PRACTICAL CHANNELS

A. Channel and system configurations

To investigate the effect of quantization and clipping caused by the ADC on various block transmission schemes, baseband equivalent simulations are conducted in Rician fading channels. The channels are simulated with the first tap fixed and the other taps following Rayleigh distributions whose variances are exponentially decaying. Two sets of channel parameters are used, consisting of Rician K-factors, tap numbers, root-mean-squared (RMS) delay spread and maximum excess delay: $\{1, 25, 7.5\,\text{ns}, 75\,\text{ns}\}$ and $\{10, 7, 1.5\,\text{ns}, 15\,\text{ns}\}$, which represent high and low level frequency selectivities of the channels. These channel parameters are taken from the measured indoor channels in the frequency band of 60 GHz configured with omnidirectional and directional antennas, respectively, see [14]. The considered constellations are QPSK and 16-QAM with Gray bit-mapping. The simulated signal bandwidth is 1.75 GHz and the data block length is $N = 1024$. The cyclic prefix is chosen to be $1/8$ of the block length so that the inter-block interference is completely resolved. In the receiver, one OFDM training symbol is used for synchronization and channel estimation.

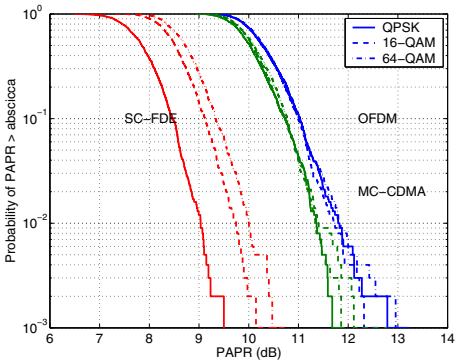

(a) $K = 1$

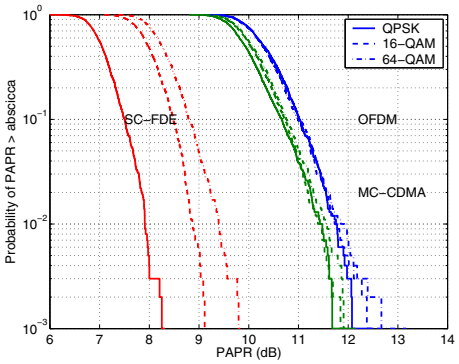

(b) $K = 10$

Fig. 2. PAPR of the noiseless received signal.

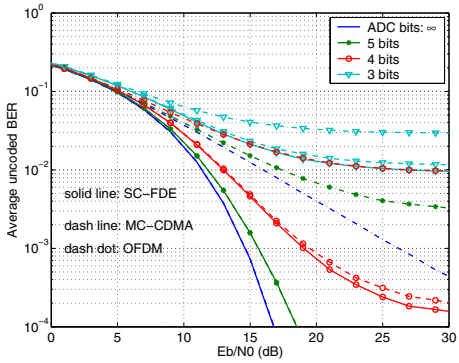

(a) QPSK

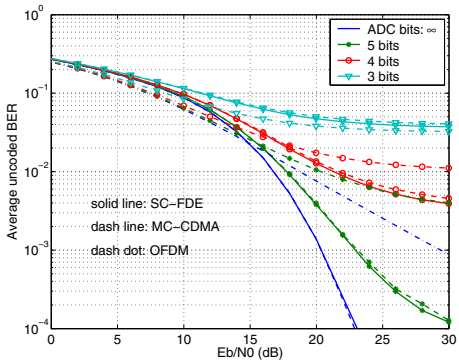

(b) 16-QAM

Fig. 3. Uncoded BER performance in Rician channel with $K = 1$.

B. PAPR

The simulated PAPR level of the received signal are depicted in Fig. 2 for the considered channel and system configurations. Here the oversampling factor is 5. Observe that the PAPRs of MC-CDMA and OFDM are relatively insensitive to channel conditions and the chosen constellation, while SC-FDE has reduced PAPRs for lower constellations and lower number of multipaths. The average PAPRs of MC-CDMA and OFDM are 10.1 and 10.3 dB, respectively. The average PAPRs of SC-FDE are $\{7.9, 8.5, 8.8\}$ when $K = 1$ and $\{7.1, 8.0, 8.3\}$ when $K = 10$ for QPSK, 16-QAM and 64-QAM, respectively. The difference in PAPR levels indicates different distributions of the received signals in the three transmission schemes. This will result in different SNR values for the decision variables as discussed in Section III-B and the differences in the simulated BER performance as shown in the next section.

C. Uncoded BER performance

The uncoded BER performance is depicted in Fig. 3 and 4 for various constellations and ADC resolutions in Rician channels with $K = 1$ and 10, respectively. With infinite ADC resolution, which corresponds to a perfect transmission without clipping and quantization, both the SC-FDE and MC-CDMA modulations show the same BER performance, which is consistent with the analysis given in Section II. In comparison with SC-FDE and MC-CDMA, OFDM always has worse performance, particularly in highly frequency channels.

Reducing the ADC resolutions results in worse performance due to increased clipping and quantization levels. More specifically, MC-CDMA has comparably the similar performance as the SC-FDE for bit resolution $R = 5$, although MC-CDMA has a much higher PAPR (see Fig. 2). The similarity of BER performance of SC-FDE and MC-CDMA indicates that frequency diversity is an effective way to reduce the impact of the quantization and clipping caused by the ADC. It also implies that the PAPR level does not always give a good indication of system performance. In case of lower ADC resolutions ($R = 4, 3$ bits), MC-CDMA performs worse than SC-FDE, particularly in channels with lower frequency selectivity. This can be explained by the fact that the clipping effect becomes much more severe for MC-CDMA. In channels with lower frequency selectivity, the larger BER difference is caused by a larger PAPR difference between the two schemes. Furthermore, the higher constellation (16-QAM) is more sensitive to the ADC effect than the lower one (QPSK).

From Fig. 3 and 4, one can see that for most cases, OFDM shows worse performance than SC-FDE and MC-CDMA, but the performance of the three schemes gets closer in cases of a near-flat channel or very low ADC resolution. An exception appears in case of $R = 3$ for 16-QAM, see Fig. 3(b), where the OFDM scheme slightly outperforms SC-FDE and MC-CDMA. Recall that each decision variable has the

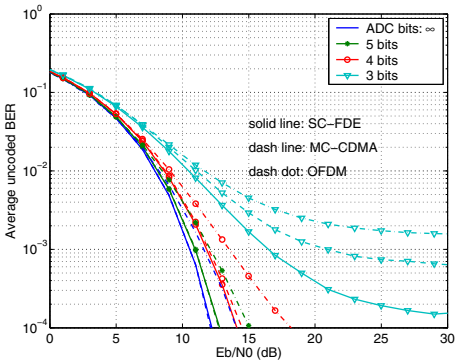

(a) QPSK

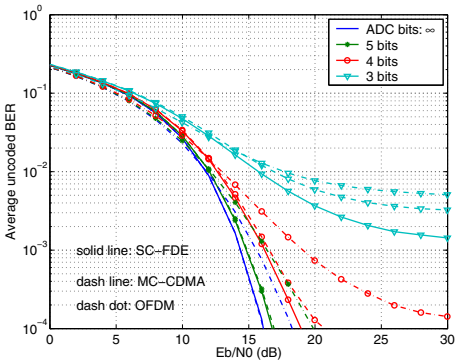

(b) 16-QAM

Fig. 4. Uncoded BER performance in Rician channel with $K = 10$.

TABLE I
THE E_b/N_0 PENALTY AT TARGET BER = 1×10^{-3} DUE TO THE ADC

Rician K-factor	ADC resolution	QPSK / 16-QAM		
		SC-FDE	MC-CDMA	OFDM
$K = 1$	5	0.9/2.2	0.9/2.7	-/-
	4	4.1/-	5.0/-	-/-
	3	-/-	-/-	-/-
$K = 10$	5	0.4/0.4	0.4/0.4	0.4/0.7
	4	1.2/1.8	1.3/2.1	1.6/2.9
	3	5.7/-	8.2/-	-/-

same SNR in SC-FDE and MC-CDMA, while in OFDM the effective SNRs of decision variables are frequency selective. Therefore, when the effective SNR of the received signal at the ADC output reaches such a low level that the probability of completely wrong detection of a full data block in SC-FDE and MC-CDMA becomes higher, while some subchannels in OFDM can still provide a sufficiently high SNR for correct detection. In this sense, OFDM is somewhat advantageous in the regime of low SNR.

By taking the required E_b/N_0 at the target BER 1×10^{-3} in linear channels (without ADC) as a reference, Table I lists the SNR penalty due to the ADC effect. When $R = 5$ and 4 bits, the three schemes have about 0.4 to 2.9 dB loss in the near-flat channels ($K = 10$), but OFDM suffers a significant loss in the near-Rayleigh channels ($K = 1$). For a lower bit ADC resolution ($R = 3$ bits), the penalty is high in both types of channels.

V. CONCLUSIONS AND DISCUSSIONS

This paper investigated the joint impact of quantization and clipping, caused by nonlinear ADCs, on SC-FDE, OFDM and MC-CDMA transmission schemes. The effective SNR of the received signal and the decision variables were derived and analyzed, where the mechanism of the ADC effect on signal detections was revealed. The joint influence on BER performance was compared for various constellations in different channel conditions. For moderate ADC resolutions ($R = 5, 4$ bits), the results showed that in practical channels, SC-FDE and MC-CDMA can achieve the same performance. As for OFDM, the performance approaches that of SC-FDE and MC-CDMA in near-flat channels and suffers less than 3 dB loss due to the low resolution ADC. In channels with severe frequency selectivity, either error correction codes or adaptive modulations might be required for OFDM to narrow the performance gap relative to the SC-FDE and MC-CDMA schemes. This leads to the conclusion that utilizing frequency diversity is effective to combat the joint effect of quantization and clipping, though not sufficient for high constellations (e.g. 16-QAM), in frequency selective channels. Moreover, for even lower ADC resolutions ($R \leq 3$ bits), the resulting performance loss is significant and it requires other solutions to combat the effects of quantization and clipping.

REFERENCES

[1] R. Fontana, "Recent System Applications of Short-Pulse Ultra-Wideband (UWB) Technology," *IEEE Trans. Microw. Theory Tech.*, vol. 52, no. 9, pp. 2087–2104, Sep. 2004.

[2] IEEE 802.15 WPAN Millimeter Wave Alternative PHY Task Group 3c (TG3c). [Online]. Available: http://www.ieee802.org/15/pub/TG3c.html.

[3] B. Widrow and I. Kollar and M. Liu, "Statistical Theory of Quantization," *IEEE Trans. Instrum. Meas.*, vol. 45, no. 2, pp. 353–361, Apr. 1996.

[4] N. Jayant and P. Noll, *Digital coding of waveforms: principles and applications to speech and video*. Prentice-Hall, Inc., 1984.

[5] J. Wepman, "Analog-to-Digital Converters and Their Applications in Radio Receivers," *IEEE Commun. Mag.*, vol. 33, pp. 39–45, May 1995.

[6] A. Nuttall, "Theory and application of the separable class of random processes," Res. Lab. Electron., M.I.T., Cambridge, MA, Tech. Rep., 1958, tech. Rep. 343.

[7] D. Dardari, "Joint Clip and Quantization Effects Characterization in OFDM Receivers," *IEEE Trans. Circuits Syst.*, vol. 53, no. 8, pp. 1741–1748, Aug. 2006.

[8] IEEE Standard 802.11a-1999, "Part 11: wireless LAN medium access control (MAC) and physical layer (PHY) specifications – amendment 1: high -speed physical layer in the 5 GHz band," Sep. 1999.

[9] ETSI, *Digital Video Broadcasting (DVB); Framing structure, channel coding and modulation for digital terrestrial television*. European Telecommunications Standards Institute, Nov. 2004, eN 300 744 V1.5.1.

[10] IEEE 802.16-2001, "IEEE Standard for Local and Metropolitan Area Networks Part 16: Air Interface for Fixed Broadband Wireless Access Systems," Apr. 2002.

[11] J. Tubbax, B. Come, L. Van der Perre, L. Deneire, S. Donnay, , and M. Engels, "OFDM versus single carrier with cyclic prefix: A system-based comparison," in *Proc. IEEE VTC'01*, Oct. 2001, pp. 1115–1119.

[12] A. Moschitta and D. Petri, "Wideband Communication System Sensitivity to Overloading Quantization Noise," *IEEE Trans. Instrum. Meas.*, vol. 52, no. 4, pp. 1302–1307, Aug. 2003.

[13] M. Sawada, H. Okada, T. Yamazato, and M. Katayama, "Influence of ADC Nonlinearity on the Performance of an OFDM Receiver," *IEICE Trans. Commun.*, vol. E89-B, no. 12, pp. 3250–3256, Dec. 2006.

[14] H. Yang and P.F.M. Smulders and M.H.A.J. Herben, "Channel Characteristics and Transmission Performance for Various Channel Configurations at 60 GHz," *EURASIP Journal on Wireless Communications and Networking, Article ID 19613*, 2007.